The Astrophysical Journal, 743:75 (11pp), 2011 December 10 doi:10.1088/0004-637X/743/1/75

THE MASS OF CoRoT-7b

Artie P. Hatzes[1], Malcolm Fridlund[2], Gil Nachmani[3], Tsevi Mazeh[3], Diana Valencia[4], Guillaume Hébrard[5], Ludmila Carone[6], Martin Pätzold[6], Stephane Udry[7], Francois Bouchy[8], Magali Deleuil[9], Claire Moutou[9], Pierre Barge[9], Pascal Bordé[5], Hans Deeg[10,19], Brandon Tingley[10,19], Rudolf Dvorak[11], Davide Gandolfi[2], Sylvio Ferraz-Mello[12], Günther Wuchterl[1], Eike Guenther[1], Tristan Guillot[13], Heike Rauer[14,20], Anders Erikson[14], Juan Cabrera[14], Szilard Csizmadia[14], Alain Léger[15], Helmut Lammer[16], Jörg Weingrill[16], Didier Queloz[7], Roi Alonso[7], Daniel Rouan[17], and Jean Schneider[18]

[1] Thüringer Landessternwarte, D-07778 Tautenburg, Germany; artie@tls-tautenburg.de
[2] European Space Agency, ESTEC, SRE-SA, P.O. Box 299, NL-2200AG, Noordwijk, The Netherlands; malcolm.fridlund@esa.int
[3] School of Physics and Astronomy, Raymond and Beverly Sackler Faculty of Exact Sciences, Tel Aviv University, Tel Aviv, Israel
[4] Observatoire de la Côte d'Azur, BP 4229, F-06304 Nice Cedex 4, France
[5] Institut d'Astrophysique de Paris, UMR 7095 CNRS, Université Pierre & Marie Curie, 98bis boulevard Arago, F-75014 Paris, France
[6] Rheinisches Institut für Umweltforschung, Universität zu Köln, Abt. Planetenforschung, Aachener Str. 209, D-50931 Köln, Germany
[7] Observatoire de l'Université de Genève, 51 chemin des Maillettes, 1290 Sauverny, Switzerland
[8] Observatoire de Haute Provence, F-04670 Saint Michel l'Observatoire, France
[9] Laboratoire d'Astrophysique de Marseille, CNRS & University of Provence, 38 rue Frédéric Joliot-Curie, F-13388 Marseille Cedex 13, France
[10] Instituto de Astrofísica de Canarias, E-38205 La Laguna, Tenerife, Spain
[11] University of Vienna, Institute of Astronomy, Türkenschanzstr. 17, A-1180, Vienna, Austria
[12] IAG, University of São Paulo, Brazil
[13] Université de Nice-Sophia Antipolis, CNRS UMR 6202, Observatoire de la Côte d'Azur, BP 4229, F-06304 Nice Cedex 4, France
[14] Institute of Planetary Research, German Aerospace Center, Rutherfordstrasse 2, D-12489 Berlin, Germany
[15] Institut d'Astrophysique Spatiale, Université Paris XI, F-91405 Orsay, France
[16] Space Research Institute, Austrian Academy of Science, Schmiedlstr. 6 A-8042, Graz, Austria
[17] LESIA, Observatoire de Paris, Place Jules Janssen, F-92195 Meudon Cedex, France
[18] LUTH, Observatoire de Paris, CNRS, Université Paris Diderot; 5 place Jules Janssen, F-92195 Meudon, France
Received 2011 April 15; accepted 2011 August 21; published 2011 November 23

ABSTRACT

The mass of CoRoT-7b, the first transiting super-Earth exoplanet, is still a subject of debate. A wide range of masses have been reported in the literature ranging from as high as 8 $M_\oplus$ to as low as 2.3 $M_\oplus$. This range in mass is largely due to the activity level of the star that contributes a significant amount of radial velocity (RV) "jitter" and how the various methods correct this jitter. Although most mass determinations give a density consistent with a rocky planet, the lower value permits a bulk composition that can be up to 50% water. We present an analysis of the CoRoT-7b RV measurements that uses very few and simple assumptions in treating the activity signal. By analyzing those RV data for which multiple measurements were made in a given night, we remove the activity related RV contribution without any a priori model. We argue that the contribution of activity to the final RV curve is negligible and that the *K*-amplitude due to the planet is well constrained. This yields a mass of $7.42 \pm 1.21\ M_\oplus$ and a mean density of $\rho = 10.4 \pm 1.8$ gm cm^{-3}. CoRoT-7b is similar in mass and radius to the second rocky planet to be discovered, Kepler-10b, and within the errors they have identical bulk densities—they are virtual twins. These bulk densities lie close to the density–radius relationship for terrestrial planets similar to what is seen for Mercury. CoRoT-7b and Kepler-10b may have an internal structure more like Mercury than the Earth.

Key words: planetary systems – techniques: radial velocities

Online-only material: color figures

1. INTRODUCTION

The discovery of the first super-Earth, CoRoT-7b, with a *measured* absolute radius and mass was recently reported (Léger et al. 2009; Queloz et al. 2009; Hatzes et al. 2010). (Currently there is no accepted definition of a "super-Earth." Here we define it as a planet having a maximum mass of $10_\oplus$.) This detection was based on the photometric measurements made by the CoRoT satellite (Convection, Rotation and planetary Transits; Baglin et al. 2006). What made this detection so interesting was that the average densities calculated from the accurate radii and radial velocity (RV) measurements of these authors all indicated values between 5.7 ± 1.3 and 9.7 ± 2.7 gm cm^{-3}. When taking the actual radius into account, these values are indicative of similar values found for the terrestrial planets in the solar system (Mercury, Venus, and the Earth), although CoRoT-7b is found much closer to its parent star.

In the exoplanet community, there has been some discussion regarding the nature of CoRoT-7b. Is this a rocky planet with a density consistent with terrestrial planets (Queloz et al. 2009; Hatzes et al. 2010), or is it a volatile-rich planet (Pont et al. 2011; Batalha et al. 2011)? The reason for this uncertainty in the possible composition is due to the wide range of planet masses that have been reported in the literature. Queloz et al. (2009) give a mass of CoRoT-7b of $m = 4.8 \pm 0.8\ M_\oplus$, Hatzes et al. 2010 report a mass of $m = 6.9 \pm 1.5\ M_\oplus$, Ferraz-Mello et al. (2011) a mass of $m = 8.0 \pm 1.2\ M_\oplus$, and Boisse et al. (2011) a mass of $m = 5.7 \pm 2.5\ M_\oplus$. While most authors favor a relatively high value for the planetary mass (and thus density) that is consistent with a rocky composition, on the low-mass end Pont et al. (2011)

[19] Also at Universidad de La Laguna, Dept. de Astrofísica, E-38200 La Laguna, Tenerife, Spain.
[20] Also at Center for Astronomy and Astrophysics, TU Berlin, Hardenbergstr. 36, D-10623 Berlin, Germany.

give a mass of $m = 2.3 \pm 1.8\,M_{\oplus}$. This low value excludes a rocky composition and can only be reconciled with relatively large amounts of volatiles (∼30% of water by mass in vapor form; Valencia 2011). Pont et al. (2011) claim that given the activity signal of the host star, the actual mass of CoRoT-7b can range from 1 to 5 $M_{\oplus}$ and thus allow a large range of bulk compositions. We thus do not know the nature of CoRoT-7b and even the detection of the planet in the RV data is marginal. They caution the reader about building models based on the rocky nature of CoRoT-7b. The perceived uncertainty of the mass of CoRoT-7b seems to linger in spite of the excellent quality of the RV measurements taken with the High Accuracy Radial velocity Planet Searcher (HARPS) spectrograph (Mayor et al. 2003). Removing this uncertainty is essential if theoreticians are to construct valid models of the internal structure of CoRoT-7b.

The reason for the wide range of mass estimates for CoRoT-7b stems from the fact that the host star, CoRoT-7 is relatively active. The CoRoT light curve shows a modulation of ≈2% with a rotation period of 23 days. This light curve also shows clear evidence of spot evolution over the 132 day observing window of CoRoT. The RV "jitter" due to activity is much larger than the expected planet signal. Further complicating the analysis is the possible presence of a second planetary companion (CoRoT-7c) with a period of 3.7 days (Queloz et al. 2009; Hatzes et al. 2010). Lanza et al. (2010) reported low-amplitude photometric variations in the CoRoT-7 light curve near the period of CoRoT-7c which would cast some doubt on the presence of this planet. However, the expected RV variations from this photometric variability is a factor of 10 less than the observed RV amplitude due to the purported planet, so activity cannot explain the entire RV variations at 3.7 days. Hatzes et al. (2010) reported the possible presence of a third companion (CoRoT-7d) with a period of 9 days. We note that the periods of CoRoT-7c and 7 days are near the sixth and fourth rotational harmonic ($P_{\rm rot}/6$ and $P_{\rm rot}/4$), respectively, so there is always the possibility that these planetary signals can arise from activity. The planet RV amplitude, central to determining the companion mass, depends on the details of how the activity signal is removed. We note that all the above mass determinations utilized the same HARPS RV data set which only emphasizes the challenge in determining the planet mass for an active star like CoRoT-7.[21]

The HARPS data used for all of these mass determinations consisted of a total of 106 precise RV measurements with a typical error of ≈2 m s^{-1} (Queloz et al. 2009) that were acquired over four months. The spectral data also produced useful activity indicators that included Ca II emission, the bisector of the cross-correlation function (CCF), and the full width at half-maximum (FWHM) of the CCF.

A variety of techniques have been employed to extract the planet RV signal from that due to activity. Queloz et al. (2009) presented two approaches. The first method used harmonic filtering of the data using the CoRoT photometric rotation period, $P_{\rm rot}$ of 23 days and its three harmonics of $P_{\rm rot}/2$, $P_{\rm rot}/3$, and $P_{\rm rot}/4$. This resulted in an amplitude of 1.9 ± 0.4 m s^{-1}. A Fourier analysis using pre-whitening (cleaning) resulted in a higher amplitude of 4.16 ± 1.0 m s^{-1}. After correcting for possible effects of the various filtering processes, a common amplitude of 3.5 ± 0.6 m s^{-1} was adopted. Ferraz-Mello et al. (2011) used a self-consistent version of harmonic filtering (denoted "high pass filtering") to get a K-amplitude of 5.7 ± 0.8 m s^{-1}. Boisse et al. (2011) also used a version of harmonic filtering of the HARPS data to derive a K-amplitude of 4.0 ± 1.6 m s^{-1}. Hatzes et al. (2010) used orbital fitting using only data from nights where more than one RV measurement was made. This resulted in a K-amplitude of 5.04 ± 1.09 m s^{-1}. One drawback to using harmonic filtering is that the orbital frequency of CoRoT-7b is close to the 1 day alias of $P_{\rm rot}/4$, so depending on the details of how the data are filtered this could influence the final RV amplitude.

[21] In terms of activity level CoRoT-7 is probably closer to that of the Sun at activity maximum rather than very active stars like T Tauri or RS CVn stars. We therefore can use solar activity as a good proxy for understanding the behavior of activity in CoRoT-7b.

Table 1
Stellar and Planetary Parameters for CoRoT-7b

Parameter	Value	Reference
Stellar mass	$0.91 \pm 0.03\,M_{\odot}$	Bruntt et al. (2010)
Stellar radius	$0.82 \pm 0.04\,R_{\odot}$	Bruntt et al. (2010)
Stellar rotational period	23.6 ± 3.2 days	Lanza et al. (2010)
Stellar age	1.2–2.3 Gyr	Bruntt et al. (2010)
Planet radius	$1.58 \pm 0.1\,R_{\oplus}$	Bruntt et al. (2010)
Planet mass	$7.42 \pm 1.21\,M_{\oplus}$	This work
Planet orbital period	0.853585 ± 0.00024 days	Léger et al. (2009)
Orbital inclination	80.°1 ± 0.°3	Léger et al. (2009)

In this paper, we present a simple approach to removing the activity signal that is model independent. We use that portion of the HARPS data that had multiple measurements per night and allow the nightly offsets to vary, following the procedure used by Hatzes et al. (2010). Here, we include four nights not used in the previous work. More importantly, we also analyze subsets of the data to see how the number of RV measurements affects the final RV amplitude (the so-called K-amplitude). We also assess the robustness of our K-amplitude determination using Monte Carlo simulations. Our analysis will help devise observing strategies to determine the K-amplitude from short-period planetary companions around active stars. This procedure confirms the high mass of CoRoT-7b and that bulk compositions consisting of up to 50% water can be reliably excluded. We compare the density of CoRoT-7b to that of the recently reported Kepler-10b (Batalha et al. 2011).

For convenience in Table 1, we summarize the basic parameters for CoRoT-7 as well as for the planetary companion.

2. DETERMINING THE K-AMPLITUDE IN THE PRESENCE OF ACTIVITY

2.1. Assumptions

Hatzes et al. (2010) used a simple method for removing the RV signal due to activity. The method exploits the fact that the RV variations due to the transiting planet have much shorter timescales than those expected from the activity signal. Only those HARPS data that had multiple measurements taken on the same night and with good time separation between successive measurements were used. This resulted in a total of 64 measurements or about one-half of the HARPS RV data (a case of less being more). (Note that this includes an additional four nights of data inadvertently left out by Hatzes et al. 2010). Table 2 lists the starting Julian Day for the nightly measurements, the number of measurements taken on that night, the time separation between first and last nightly measurement, and the resulting orbital phase difference between the first and last observation on that night.

There are two very simple assumptions in this analysis: (1) a 0.85 day RV period is present in the data. (2) The RV zero-point

Table 2
Journal of Observations

Start	N_{obs}	ΔT (hr)	$\Delta\phi$	$\Delta V_{C7c,d}$ (m s^{-1})
2454799.7770	2	2.10	0.10	−0.33
2454800.9461	2	2.09	0.10	0.05
2454801.7530	2	2.08	0.10	0.76
2454802.7484	2	2.27	0.11	−0.45
2454803.7526	2	1.95	0.09	−0.95
2454804.7554	2	1.75	0.09	−0.07
2454805.7775	2	1.75	0.09	−0.35
2454806.7647	2	1.91	0.09	−0.42
2454807.7281	2	2.36	0.12	−0.18
2454847.5968	3	3.84	0.19	−1.63
2454848.6008	3	3.80	0.19	−0.78
2454849.5940	3	3.72	0.18	0.76
2454850.5951	3	3.72	0.18	−0.52
2454851.5927	3	3.72	0.18	1.19
2454852.7986	3	3.42	0.17	−0.17
2454853.5740	3	4.13	0.20	2.00
2454854.5802	3	3.88	0.19	−0.27
2454865.5978	2	2.83	0.14	0.01
2454867.5604	2	2.30	0.11	0.17
2454868.5918	2	2.30	0.11	0.32
2454869.6002	2	2.11	0.10	−0.63
2454870.6013	2	2.75	0.13	−0.07
2454872.5647	3	3.91	0.19	−1.43
2454873.5375	3	4.38	0.21	0.96
2454879.6002	2	3.35	0.16	1.33
2454882.5256	2	3.11	0.15	1.16
2454884.5265	2	2.87	0.12	−1.43

offset does not vary significantly over the span of measurements for a single night.

Assumption (1) is reasonable given the clear transit signal in the data. Léger et al. (2009) carefully excluded all possible false positives and established with a high degree of confidence that a planetary companion was causing the transit event. Hatzes et al. (2010) showed that even this assumption can be relaxed as the 0.85 day period provides the best fit to the data. Later we show a periodogram analysis that also confirms that a 0.85-d period provides the best fit to the RV data.

Assumption (2) is also eminently reasonable. The rotation period is known to be 23 days and over the time span of the nightly observations (maximum ≈4 hr) the star rotates by no more than 2.°6. The RV amplitude due to activity rotational modulation is ≈10 m s^{-1} (Queloz et al. 2009). This means that the change in RV due to rotational modulation will amount to a *maximum* value of < 0.5 m s^{-1}. This is less than the expected change in the RV due to the orbital motion of CoRoT-7b which is 1–5 m s^{-1} and with an average of about 3 m s^{-1} on a given night. Rapid and significant changes in the spot distribution on timescales of ≈4 hr in a star with solar-like activity like CoRoT-7 would be unprecedented. For instance, measurements of the solar constant from the Solar Maximum Mission shows peak variations of 0.2% on timescales only as short as *weeks* (Foukal 1987), i.e., much longer than the timescales of our nightly variations or the orbital period of CoRoT-7b. Photometric variability does not necessarily translate into RV variability and vice versa, but drawing from the solar analogy we do not expect significant activity related RV variations on timescales of a few hours. In short, we expect that the RV contribution due to activity over the time span of the nightly measurements should be nearly constant.

If there are additional planets present then these might contribute to changes in the mean RV for a given night that would not subtract out fully. These, however, also make a negligible contribution. For the sake of argument let us *assume* that CoRoT-7c and CoRoT-7d are also present. Using the orbital solutions of Hatzes et al. (2010), we can calculate the change in RV on a given night due to the reflex motion of the star caused by these companions. This is listed in the fifth column of Table 2 under $\Delta V_{C7c,d}$. (Note that due to the shorter period the largest effect stems from CoRoT-7c.) The average change in RV is −0.04 with an rms scatter of only 0.89 m s^{-1}. The maximum change in RV of 2 m s^{-1} only adds a maximum possible error of ±1 m s^{-1} to the zero-point offset. For most nights, the error is less than 0.5–1 m s^{-1}. Combined with the rotational modulation signal, the error in the nightly RV zero-point offsets (mean values) is less than the measurement error of about 2 m s^{-1} as well as the typical change in the RV due to orbital motion. We should emphasize that it is irrelevant whether CoRoT-7c and CoRoT-7d exist or not. If they are actually caused by stellar activity then our orbital solution can be treated as a "model" for this activity that still provides a good estimate for the short-term activity RV jitter.

We stress that in this procedure we essentially do not care what the contribution of surface spots or other planets is to the RV signal. By calculating the mean RV value for a given night (in a least-squares sense) and subtracting this from the signal, we effectively remove all other contributions to the RV signal that have periods substantially longer than the orbital period of CoRoT-7b. Our approach will also remove any unknown long-term systematic instrumental errors that may be present. The stability of the HARPS spectrograph is nearly legendary with nightly drifts of the spectrograph on average being less than 0.5 m s^{-1} (Lo Curto et al. 2010). Even if HARPS had night-to-night systematic errors, our approach should eliminate, or at least greatly minimize these. As long as the RV variations from other sources do not change significantly over a 2–4 hr time span, any RV variations that are seen in a given night can be attributed solely to that of CoRoT-7b.

2.2. Nonlinear Least-squares Fitting

An orbital solution was made using the generalized nonlinear least-squares program *Gaussfit* (Jefferys et al. 1988) and treating data from individual nights as independent data sets with their own velocity (γ-velocity) offset. (For convenience, we refer to this as the "model-independent" approach.) Such a technique has been used successfully to compute orbital solutions by combining multiple RV data sets taken with different instruments and using different RV measurement techniques (for example, see Hatzes et al. 2003). The period was fixed to the CoRoT-determined transit value of 0.853585 days, but the phase, amplitude, and nightly offsets were allowed to vary until the best-fit solution was found that minimized the χ^2. The calculated phase reproduced the transit phase to within 0.01. Varying the orbital eccentricity resulted in a small eccentricity ($e = 0.077$) but with large errors (±0.11). The orbit can be considered to be circular. For the final solution, we used a zero eccentricity and fixed the orbital phase to the transit value.

Figure 1 shows the nightly RV measurements after removal of the nightly zero-point offsets and phased to the CoRoT transit ephemeris. The resulting K-amplitude is 5.15 ± 0.95 m s^{-1}. Measurements taken in a single night are represented by the same symbol and one clearly sees that the change in the RV almost always follows the orbit to within the measurement error.

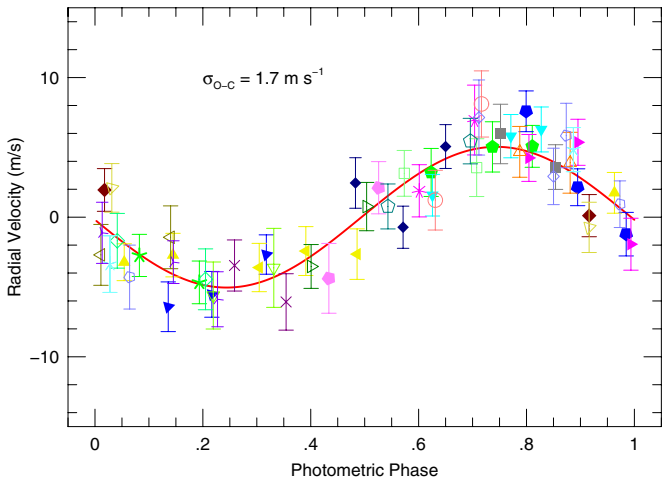

Figure 1. RV measurements for CoRoT-7b taken on the 27 nights listed in Table 1. On these nights, multiple observations were made separated by 2–4 hr. Values are phased according the CoRoT transit phase. Different symbols represent measurements for different nights. The line represents the orbital solution.

(A color version of this figure is available in the online journal.)

The rms scatter of the RV data about the orbital solution (line) is 1.68 m s^{-1} which is in excellent agreement with the median RV internal error of 1.77 m s^{-1}. This figure alone argues that the contribution of activity jitter to this RV curve is negligible.

We also see no obvious evidence for any short-term (i.e., during the night) systematic errors in the RV data (possible long-term errors are removed by subtracting the nightly mean), otherwise we would see a scatter about the orbital solution significantly larger than the typical measurement error. There are several dozen cases where the RV measurements of stars are in the same signal-to-noise regime as CoRoT-7 and these show a residual scatter in the range of 1.5–3.5 m s^{-1} (Naef et al. 2010; Lo Curto et al. 2010; Moutou et al. 2011), comparable to what we see in CoRoT-7.

2.3. Linear Model

Our Keplerian solution from the previous section established that the orbit of CoRoT-7b is circular and in phase with the transit light curve. We can thus use a *linear* model of the form:

$$A\cos(\omega t_i) + B\sin(\omega t_i) + C_i, \quad (1)$$

where A and B determine the amplitude and phase of the sine function fitted to the RV periodic modulation, and $C_i \in \{C_1, \ldots, C_{27}\}$ are the different shifts for each of the 27 nights with multiple measurements (each C_i is assumed to be constant for each night), $\omega = 2\pi/P$ for a given period P and t_i is the time of each measurement. Presenting the model in the form of Equation (1) enabled us to apply a linear model to the data as the phase does not appear explicitly thus assuring a robustness of the best solution. The resulting RV amplitude from the linear model was 5.25 $\pm$0.84 m s^{-1}, entirely consistent with the *Gaussfit* result. We shall use this value as our "best-fit" K-amplitude. In order to assess the significance of the detected periodicity, we applied the linear model to the RV measurements using a range of different frequencies, to see weather our analysis detected any modulation with another periodicity. The periodogram of derived $1/\chi^2$ as a function of frequency in the range (0,2] day^{-1} (Figure 2) shows a clear global maximum near CoRoT-7b's period, which was found through photometry by Léger et al. (2009).

We also performed a bootstrap test to see if random data can produce the same modulation. In the test, all RVs used in the analysis were randomly shuffled, leaving the observing times the same. We performed 100,000 runs, each contained 1000 frequencies at the same range taken in the periodogram of Figure 2. Out of 10^8 linear fits, the highest $1/\chi^2$ value was 0.24, while the original data yielded a maximum $1/\chi^2$ of 1.2, near the Corot-7b period. The results are plotted in Figure 3, which

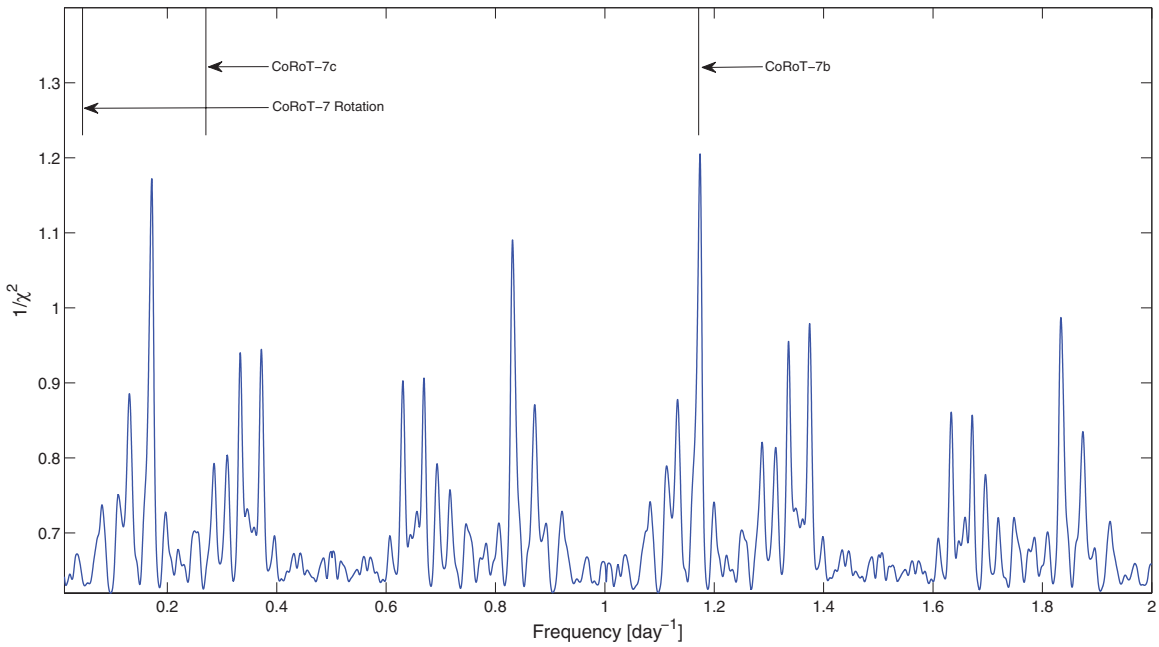

Figure 2. Periodogram of $1/\chi^2$ vs. frequency using the linear model. The highest peak is clearly at Corot-7b frequency. The next two highest peaks are alias frequencies of Corot-7b around 1 and 0.5 day^{-1}. The frequencies corresponding to CoRoT-7c and the rotation period are also marked. There is no peak at these two frequencies.

(A color version of this figure is available in the online journal.)

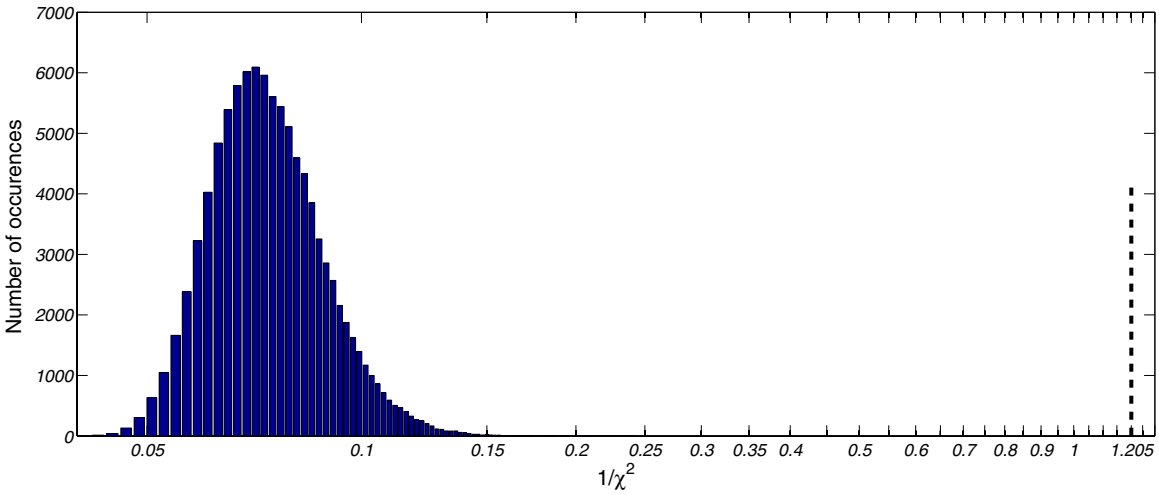

Figure 3. Histogram of the values of the highest peaks of the $1/\chi^2$ periodograms of 100,000 bootstrap random sets of data. The value of the peak of the real data is also marked.

(A color version of this figure is available in the online journal.)

shows a histogram of the highest $1/\chi^2$ values for all 100,000 runs. We conclude that the RV modulation with the photometric period was detected with a significance higher than 10^{-5}.

2.4. Finite Differences

The finite differences of the nightly RV measurements can also be used to estimate a *K*-amplitude that is largely insensitive to the contribution of the activity. Differences (derivative) should remove the underlying activity signal assumed to be constant for a given night so that any changes in the RV can be attributed solely to orbital motion. The fitting to the RV data done in the previous sections confirms that the orbit is circular and in phase with the CoRoT ephemeris. The RV curve can thus be described by the function: $V = -K\sin(2\pi\phi) + C_i$, where K is the RV amplitude, ϕ the orbital phase, C_i is the nightly zero point, and the "minus" sign ensures that the RV curve has the proper phase with respect to the mid-transit time. Differentiating with respect to ϕ results in $dV/d\phi = -2\pi K\cos(2\pi\phi)$. So, a plot of the derivative (differences) of the RV values versus $\cos(\phi)$ should have a linear relationship whose slope is proportional to the *K*-amplitude.

Figure 4 shows the normalized nightly RV derivatives $(dV/d\phi/2\pi)$ as a function of $-\cos(\phi)$. There is considerable scatter since we are dealing with differences, but there is a clear correlation. The correlation coefficient is $r = 0.59$ with a probability of 6×10^{-5} that the data are uncorrelated. A least-squares fit to the derivatives yields a *K*-amplitude of 5.02 ± 1.25 m s^{-1} a value entirely consistent with the previous approaches.

Since the derivative of a circular orbit is also a trigonometric function one should also be able to fit a sine function (with the proper phase) to the finite differences. Doing this resulted in a *K*-amplitude of 6.09 ± 1.42 m s^{-1}. In summary, the finite difference also demonstrates the presence of nightly variations consistent with a period of 0.85 day and a *K*-amplitude of $\approx$5 m s^{-1}.

2.5. Robustness of K-amplitude Determination

We assessed the robustness of our *K*-amplitude determination through a series of tests. First, we investigated how the calculated *K*-amplitude depended on the amount of data that was used. The top of Figure 5 shows the *K*-amplitude as a function of number of nights of data used in the solution. After five nights of data,

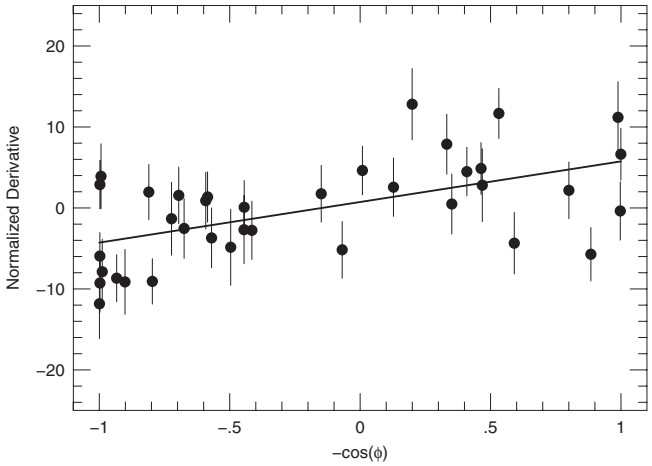

Figure 4. Normalized derivative, $(dV/d\phi)/2\pi)$ calculated from successive RV measurements plotted vs. the negative of the cosine of the orbital phase. The data have a correlation coefficient of $r = 0.59$ and with the probability of 6×10^{-5} that they are uncorrelated. The slope corresponds to an RV amplitude of $K = 5.02 \pm 1.26$ m s^{-1}.

the *K*-amplitude converges to within the errors to the nominal value using all the data (horizontal dashed line). The final two points at the right show the *K*-amplitude determined using those nights with only two measurements ($K = 4.00 \pm 1.56$ m s^{-1}) and nights with three measurements ($K = 5.87 \pm 1.21$ m s^{-1}). Both agree to the nominal value within the errors.

We also performed Monte Carlo simulations to confirm the error on the *K*-amplitude, but more importantly to assess how well we could recover a known signal in the RV data. Given the relative sparse sampling of the sine curve on each night, there was some concern that when fitting a fixed period to the data the procedure may introduce variations with that period into the data due primarily to the freedom in varying the nightly offsets. A synthetic sine wave was generated with an amplitude of 5 m s^{-1} and having the same period and phase of CoRoT-7b. The fake data were sampled in the same manner as the real data and random noise at a level of 2 m^{-1} were added. To mimic the activity signal, random noise with an rms of 10 m s^{-1} was added to the fake RVs for each night. The data were then processed in the same manner as the real data. One hundred

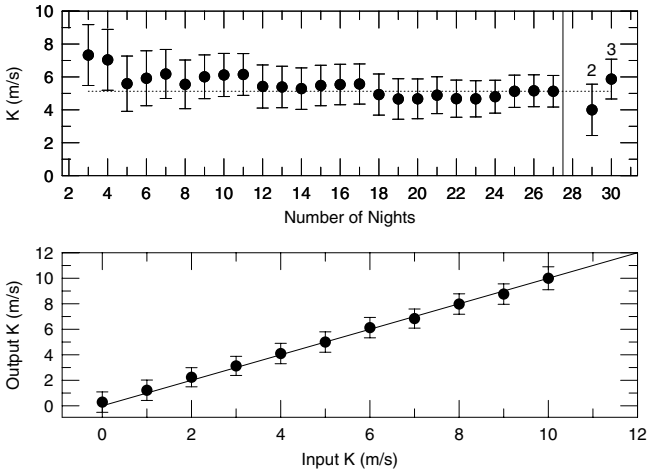

Figure 5. Top: the derived *K*-amplitude as a function of the number of nights used in the solution. The horizontal line represents the best-fit amplitude using all the data. The last two points (left of the vertical line) represent the *K*-amplitude determined using only data with two measurements per night (labeled "2") and nights with only three measurements (labeled "3"). Bottom: simulations using a sine function sampled in the same manner as the data and with random noise consistent with the HARPS median error (1.8 m s^{-1}) added. For each night, a random offset of up to ±10 m s^{-1} was added to the nightly values to mimic the activity jitter. The abscissa is the input *K*-amplitude and the ordinate the output *K*-amplitude. Each point represents an average amplitude of 20 synthetic data sets generated with the same amplitude, but different random numbers. The line represents unity slope.

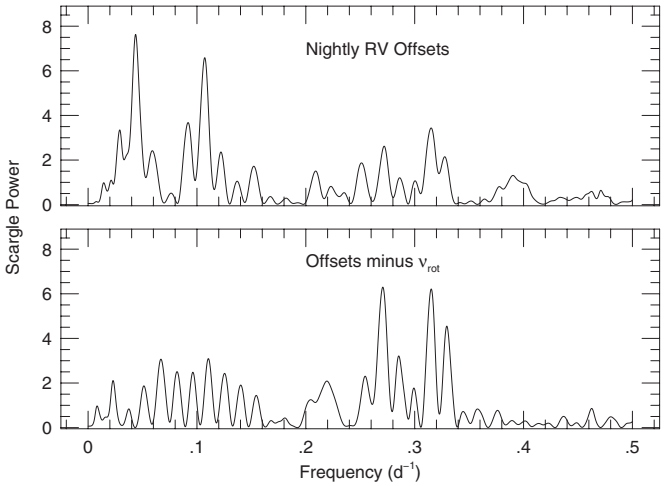

Figure 6. Top: the Scargle periodogram of the nightly offsets that were determined in the orbit fitting. The peak corresponds to the stellar rotational frequency of 0.043 *c* d^{-1}. Bottom: the Scargle periodogram of the offset residuals after removing the contribution of the dominant peak.

such simulations yielded a mean amplitude of 5.00 ± 0.94 m s^{-1} and in all cases the nightly "activity" signal was recovered to within the measurement error. The error in the *K*-amplitude from the simulations is entirely consistent with the measured value and suggests that the errors in the RV measurements are nearly Gaussian. The procedure also is able to recover the input amplitude over a wide range of input *K*-amplitudes (0–10 m s^{-1}) as shown in lower panel of Figure 5. Each point in this figure represents an average amplitude from 20 simulated data sets.

The previous simulations assumed a random component to the underlying activity signal. However, this component is most likely periodic and we should worry about the activity related RV variations with a frequency of four times the rotational frequency, $4\nu_{\rm rot}$ since this may correlate with an 0.85 day period through the 1 day alias (see below). This might introduce a significant contribution to the recovered *K*-amplitude. As a final test, we used a sine wave with a period of one-fourth the rotation period to provide the value for the constant RV offset due to activity. A discrete Fourier transform (DFT) of the raw HARPS RV data yields an amplitude of 4.6 m s^{-1} near $4\nu_{\rm rot}$. Although this is mostly due to the 1 day alias of the orbital frequency of CoRoT-7b, we used this as a "worst case scenario" for the contribution to the activity signal due to $4\nu_{\rm rot}$. An input amplitude of 5 m s^{-1} was then used for planet *K*-amplitude and the phase of the underlying "activity" sine wave was varied over the full range (0–2π). The recovered *K*-amplitude ranged from 4.6 to 5.6 m s^{-1}, i.e., within the error of our nominal value. We conclude that we can reliably recover the *K*-amplitude of CoRoT-7b even in the presence of activity that is correlated with the rotational period.

3. THE ACTIVITY SIGNAL

3.1. Rotational Modulation

The nightly RV offsets calculated by our procedure should have some relationship with the underlying activity signal which should be dominated by the rotation period. To check this, we performed a Scargle periodogram (Scargle 1982) on the calculated nightly offsets. This periodogram, shown in Figure 6, has its highest peak at a frequency of $\nu = 0.043 \pm 0.002$ *c* d^{-1} which is consistent with the rotational frequency for the star of 0.0423 ± 0.006 *c* d^{-1} from Lanza et al. (2010). According to Scargle (1982), the probability that noise will produce this peak exactly at the rotational frequency is about 5×10^{-4}. This was confirmed using a bootstrap randomization procedure. The RV data were randomly shuffled 200,000 times, keeping the times fixed and the maximum power in the random data periodogram was examined. Over the narrow frequency range 0.035–0.055 *c* d^{-1} centered on the rotational frequency, the false alarm probability that noise is causing the observed peak was 7×10^{-5}. The derived nightly offsets thus have some relationship to a known phenomenon associated with the star (i.e., rotation)—these are not arbitrary. The RV amplitude of this peak is ≈10 m s^{-1}, consistent with the RV amplitude due to rotational modulation using the entire HARPS data set (Hatzes et al. 2010).

3.2. The Bisector and FWHM Variations

Queloz et al. (2009) used a method similar to that of this paper to study the possible variations of the CCF bisector induced by the RVs variations due to the CoRoT-7b signal. For each of the observing nights with two or three measurements per night, they corrected the RVs from their average during the night over the two or three measurements. They did the same correction on the bisector span by their nightly average. These "differential" bisector spans and RVs can show short-period variations, on a timescale of about 5 hr which is the typical longest time offset between data on nights with multiple observations. This represents 25% of the CoRoT-7b orbit.

The nightly variations of the bisector span as a function of the nightly variations of the RVs are plotted in Figure 7. It shows peak-to-peak variations on the order of 20 m s^{-1} for the bisector spans and 10 m s^{-1} for the RVs. The larger dispersion of the bisectors agrees with their error bars that are twice as large as than those for the RVs. The bisectors show a hint for correlation with the RVs. With the hypothesis of a linear correlation, the data show a positive slope of 0.45 ± 0.22 that is plotted in Figure 7.

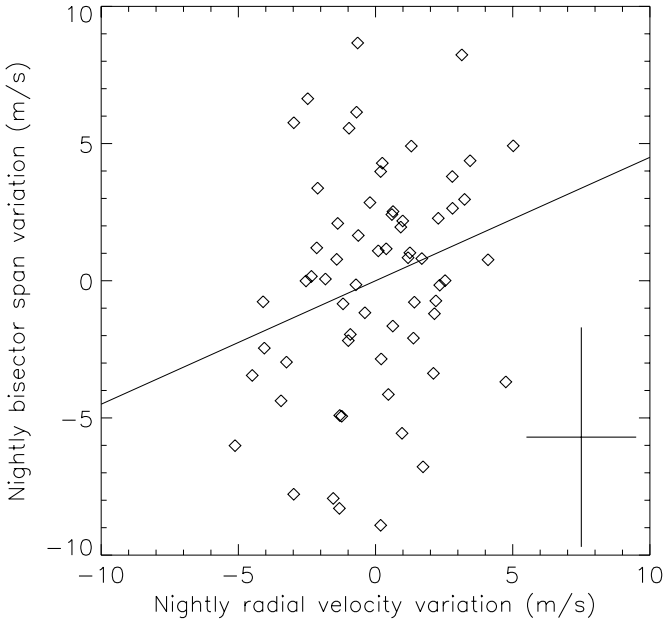

Figure 7. Bisector spans as a function of radial velocities (RV; nightly variations). For each observing night, both bisector spans and RVs are corrected for the average value of the night. The typical error bars on each point are plotted in the bottom right. There is a 2σ hint for the detection of a correlation between the bisector spans and the RVs. The linear correlation has a slope of 0.45 ± 0.22 that is shown on the plot.

The Spearman's rank test indicates a 2σ deviation from the null correlation hypothesis. A bootstrap with 30,000 pools mixing RV and bisectors shows a slope distribution centered on zero, with only 1.9% probability to find a slope of 0.45 or larger. It also shows a 2.1% probability to find by chance a deviation from the null correlation hypothesis greater than 2σ with the Spearman's test.

Thus, the data show a 2σ detection of a positive correlation between the differential bisector spans and RVs, on a night-per-night basis. Such correlation could be the signature of a blend scenario (e.g., Santos et al. 2002), where a star in the background of the main target hosts a deep transit which seems shallower as it is diluted by the constant, brighter flux of the main target. However, blend simulations presented by Queloz et al. (2009) have shown that the slope of the bisector versus the RV should be steeper than 2 in all cases, whereas 0.45 ± 0.22 is found here. Thus, the possible correlation between bisector spans and RVs apparently cannot be explained with a blend scenario. In addition, such a blend scenario would have to imply that the background star hosts a deep transiting companion while the main star, by chance, hosts at least one planet (CoRoT-7c) as detected in RVs. A planetary system is more likely with the two companions orbiting the same stars.

To investigate further any possible bisector variations, the same analysis using *Gaussfit* that was applied to the RV data was also applied to the bisector data. Namely, the nightly data were treated as independent data sets and a sine wave was fit to the data keeping the period fixed at 0.85 days and allowing the nightly means to float. If we find strong sinusoidal variations with a 0.85 day period it would imply that either that activity is contributing significantly to the RV signal, or that our procedure is introducing RV variations with the planet orbital period. The top of the Figure 8 shows the residual bisector variations after subtracting the calculated nightly mean and phased to the CoRoT-7b period. There is no compelling evidence for

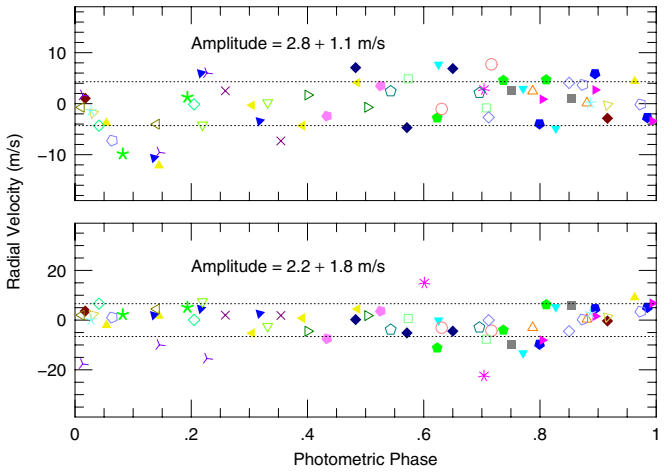

Figure 8. Top: the residual bisector variations resulting from performing the same analysis as done on the RV data and phased to the photometric period. The dashed horizontal lines represent the $\pm 1\sigma$ calculated for the data in the phase interval 0.15–1.0. Bottom: the residual FWHM resulting from performing the same analysis as done on the RV data phased to the photometric period.

(A color version of this figure is available in the online journal.)

sinusoidal variations. A sine fit to the data yields an amplitude of 2.8 ± 1.1 m s^{-1}. The only hint of variability is driven by a cluster of only four points at phase $\approx$0.1. Eliminating these points in a much lower amplitude of 1.6 ± 0.9 m s^{-1}. Most of the bisector span data between phases 0.2 and 1.0 have an rms scatter of $\pm 1\sigma$ as shown by the dashed lines. For now any possible bisector correlation or variations remain unexplained, but one should keep in mind that these variations with the present data set do not seem to be significant. Even though there are often large nightly variations, these are all within the rms scatter of about 4.5 m s^{-1}. (Compared to the $\approx$10 m s^{-1} rms scatter for the bisector variations of Kepler-10b, see Figure 7 of Batalha et al. 2011.) This also argues against any possible variations being due to a blend scenario.

We also applied this method to the FWHM measurements. This is shown in the bottom panel of Figure 8 where we plot the FWHM residuals phased to the 0.85 day period. The amplitude of any variations is 3.8 ± 3.2 m s^{-1}. There is no strong evidence for variability in the FWHM with a 0.85 day period.

3.3. Contribution of Activity to the K-amplitude

There are two possibilities for the RV curve shown in Figure 1: either it is dominated by the reflex motion of the star due to CoRoT-7b, or the signal due to activity is producing a significant contribution to the amplitude. Pont et al. (2011) derived a significantly lower *K*-amplitude of 1.6 ± 1.3 m s^{-1} after employing their model for the activity on CoRoT-7. If this value is correct, then this implies that a significant contribution (about 3.5 m s^{-1}) to the RV amplitude comes from the contribution of activity.

The striking feature about the RV curve (Figure 1) is that it does not deviate from a circular orbit (i.e., pure sine curve) to within the errors *using the period and phase of the photometric transit*. Naively, we would expect an uncorrected activity signal to distort significantly the RV curve—it should not be so "clean." We believe that the stellar activity actually contributes little to the observed RV amplitude.

For activity to contribute significantly to the RV curve, it would have to have variations that would mimic the 0.85 day period and be *perfectly in phase with the CoRoT-7b lightcurve*

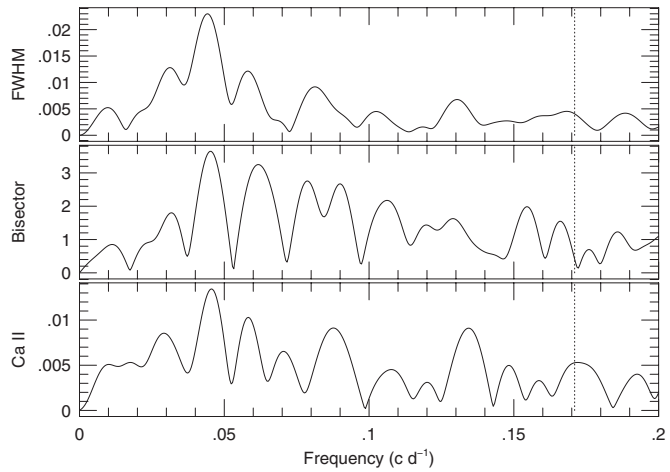

Figure 9. Amplitude spectrum of the FWHM (top), bisectors (middle), and Ca II emission (bottom) calculate using the discrete Fourier transform. The vertical dashed line marks the location of the $4\nu_{\rm rot}$ which is the 1 day alias of the orbital frequency of CoRoT-7b.

ephemeris, otherwise we could not fit a circular orbit to the data. We could concoct a spot distribution that evolves with just the right timescales and phase with respect to the 0.85 day period, but that would be too ad hoc and lacking in a reasonable physical interpretation. The simplest and most logical way to produce a 0.85 day variation in the RV data, and one that has a stronger physical basis, is with the 1 day alias of $P_{\rm rot}/4$ ($\nu = 4\nu_{\rm rot} + 1$) which is close to the CoRoT-7b orbital frequency. We emphasize that Figure 8 of Hatzes et al. (2010) and the periodogram in Figure 2 demonstrate that the true period of 0.85 day is favored over the alias period and that it provides a better fit to the data. However, for the sake of argument let us assume that a large part of the RV amplitude in Figure 1 is indeed due to an alias of $4\nu_{\rm rot}$ rotational harmonic. We argue that this cannot be the case for two strong reasons.

First, there is little evidence for $4\nu_{\rm rot}$ actually being present in the activity indicators. Assuming the Pont et al. *K*-amplitude of 1.6 m s^{-1} is indeed correct, then ≈3.5 m s^{-1} of the RV amplitude has to be accounted for by activity. The RV amplitude associated with the rotational frequency is 8.7 m s^{-1}. This means that the fourth harmonic ($\nu_{\rm rot}$) should have an amplitude ≈0.4 of the rotational peak. We find, however, weak evidence for significant power at $4\nu_{\rm rot}$. Figure 9 shows the DFT amplitude spectra of the FWHM, the bisectors, and the Ca II emission. The vertical line marks the location of $4\nu_{\rm rot}$ which is near the 1 day alias of the orbital frequency of CoRoT-7b. Only the FWHM and Ca II show a bit of power near this rotational harmonic. The FWHM shows a ratio of the fourth harmonic to rotational frequency of only 0.2. Ca II does show a peak at the third harmonic with the proper amplitude (≈0.4). However, the DFT of both the FWHM and bisector span are quite noisy with other peaks close to the fourth harmonic having a larger amplitude. Pont et al. (2011) argue that the FWHM can be used to reconstruct the brightness variations to 0.1% or better. If this is true, and since $4\nu_{\rm rot}$ has an amplitude 20% of the rotational peak, then the RV variations due to the fourth harmonic should be about 1.7 m s^{-1}, or comparable to the measurement error.

Second, and just as importantly, we would have to place very stringent constraints on the spot distribution and its evolution that are highly unlikely:

1. Physically, the only way to produce a strong presence of $P_{\rm rot}/4$ in the RV rotational modulation is to have four spot groups equally spaced in longitude by 90°. Each spot group would produce its own sinusoidal variation and all four RV curves from the individual spot groups would add together to contribute to the observed 0.85 day RV variations (in this case, the 1 day alias of $P_{\rm rot}/4$.)
2. For activity to reproduce the CoRoT transit phase and to be able to add or subtract to the RV curve in the proper phase, one spot group *must be located at transit phase zero*. Otherwise, the activity signal would introduce significant distortions to the RV curve. We cannot dismiss that the close proximity of the planet actually influences the stellar activity and spot alignment. However, the evidence for such star–planet interaction is weak. Shkolnik et al. (2005, 2008) did find hints of planet related chromospheric activity in HD 179949 and υ And. Scharf (2010) found a correlation between X-ray luminosity and the presence of massive, close-in planets. However, Poppenhaeger et al. (2011) could not find any variations in Ca II and X-rays that could be traced back to the planet in υ And. Furthermore, Poppenhaeger et al. (2010) find that the correlation between X-rays and planet hosting stars can be attributed to selection effects and that in fact no correlation is seen. Thus, there is no compelling observational evidence that the presence of close-in planetary companions influences the activity on the star. Furthermore, these results were for giant planets much more massive than CoRoT-7b. It is not clear how a very low mass planet can influence the activity of the star.
3. To produce the symmetrical RV curve in Figure 1 and with little scatter, all four spot groups must have comparable filling factors, otherwise the envelope of RV curves from the individual spot groups would introduce significant "jitter" and the observed scatter of the RV data would exceed the measurement errors. For example, this is seen in the RV curve for Kepler-10 (Batalha et al. 2011) where the assumed RV jitter dominates the internal measurement error in spite of this star being "quiet" in terms of activity. This filling factor can be estimated using the expression of Hatzes (2002) or Saar & Donahue (1997). To produce a spot-induced RV amplitude of 5 m s^{-1} requires a spot filling factor for each group of about 0.3%. The difference in spot filling factor (areal coverage) can be estimated from the rms scatter about the orbital solution. For the RV curves from the different spot groups to produce variations less than the rms scatter of $\sigma = 1.68$ m s^{-1}, they must have the same filling factors to within 70%. Using binned RV values (approximately 5–10 points per bin) in order to minimize the measurement error (≈2 m s^{-1}), one gets an rms scatter of 0.5 m s^{-1}. In this case, the spot-filling factors for all spot groups must be the same to within about 10%.
4. A symmetrical RV curve also implies that the spot evolution over the span of the measurements for all four spot groups must be small. The RV measurements span more than 3.5 rotation periods and as noted by Pont et al. (2011): "no feature is reproduced unchanged after one rotation period, and the light curve becomes unrecognizable after merely 2–3 periods." Having four spot groups that evolve very little over 3.5 rotation periods seemingly contradicts what we see in the light curve of CoRoT-7b.

So, either we have a star with a super-Earth planet (similar to Kepler-10b—see below), or we have a star with a remarkable spot distribution. We thus conclude that the 0.85 day RV modulation seen in Figure 1 is due almost entirely to the reflex motion induced by a planet. Taking all the arguments into

Table 3
Mass Determinations for CoRoT-7b

N	*K*-amplitude (m s^{-1})	Mass ($M_\oplus$)	Method	Reference
1	5.70 ± 0.80	8.0 ± 1.20	High pass filtering	Ferraz-Melo et al. (2011)
2	5.15 ± 0.95	7.29 ± 1.35	Model independent	This work
3	5.27 ± 0.81	7.46 ± 1.16	Linear model	This work
4	5.04 ± 1.09	7.12 ± 1.43	Offset fitting	Hatzes et al. (2010)
5	4.16 ± 1.00	5.88 ± 1.49	Pre-whitening	Queloz et al. (2009)
6	4.00 ± 1.60	5.65 ± 1.61	Harmonic filtering	Boisse et al. (2011)
7	3.80 ± 0.80	5.37 ± 0.82	Harmonic filtering w/correction	Queloz et al. (2009)
8	3.50 ± 0.60	4.96 ± 0.86	Adopted	Queloz et al. (2009)
9	3.33 ± 0.80	4.70 ± 1.40	Pre-whitening w/correction	Queloz et al. (2009)
10	1.90 ± 0.40	2.65 ± 0.56	Harmonic filtering	Queloz et al. (2009)
11	1.60 ± 1.30	2.26 ± 1.83	Activity modeling	Pont et al. (2011)

account, the most reasonable, and most logical, explanation for the 0.85 day RV variations of CoRoT-7 is that these are entirely due to the transiting planet, CoRoT-7b. Furthermore, the significance of this detection is at the 15σ level.

4. DISCUSSION

4.1. The Mass of CoRoT-7b

The planet mass can be derived from the *K*-amplitude via the mass function, $f(m)$ which for circular orbits (the most likely case for CoRoT-7b) is

$$f(m) = \frac{(m_p \sin i)^3}{M_{\rm star}^2} = \frac{K^3 P}{2\pi G}, \quad (2)$$

where P is the orbital period, $M_{\rm star}$ is the stellar mass, and G is the gravitational constant. Bruntt et al. (2010) derived a stellar mass of $0.91 \pm 0.03\, M_\odot$ and Léger et al. (2009) derived an orbital inclination of $i = 80.^\circ1 \pm 0.^\circ3$. Using the appropriate stellar and orbital parameters for CoRoT-7b and solving Equation (1) for m_p results in $m_p\,(M_\oplus) = (1.416 \pm 0.031)K$ (m s^{-1}). Our best-fit *K*-amplitude of 5.25 ± 0.84 m s^{-1} (linear model) results in $m = 7.42 \pm 1.21\, M_\oplus$.

Table 3 lists all the different *K*-amplitude determinations for CoRoT-7b from here and the literature. For Queloz et al. (2009), we include not only the adopted value but also the results from the individual methods for determining the RV amplitude. To ensure that the mass was determined in a consistent way using the same stellar and orbital parameters, we recalculated these using the published *K*-amplitudes and the mass function. These may result in slightly different values than quoted in the respective papers. These appear in the third column in the table and graphically in Figure 10. The number on the abscissa corresponds to that in the first column of the table. Our mass for CoRoT-7b agrees to within 1σ to most other mass determinations. It is most discrepant (4σ) with the harmonic filtering without correction from Queloz et al. (2009), but the authors showed that the filtering process resulted in an unusually low value. The authors considered the adopted value of 4.96 ± 0.86 to be a more accurate determination.

Our mass value is clearly discrepant with the low value of $2.3 \pm 1.8\, M_\oplus$ ($\sim 1\sigma$) claimed by Pont et al. (2011), a mass determination largely responsible for casting doubt on the rocky nature of CoRoT-7b (Batalha et al. 2011). The results of Pont et al. were based on a rotating, time-evolving spot model consisting of 2–200 spots with their own latitude, longitude, and scale factor (i.e., temperature). Solar-like differential rotation

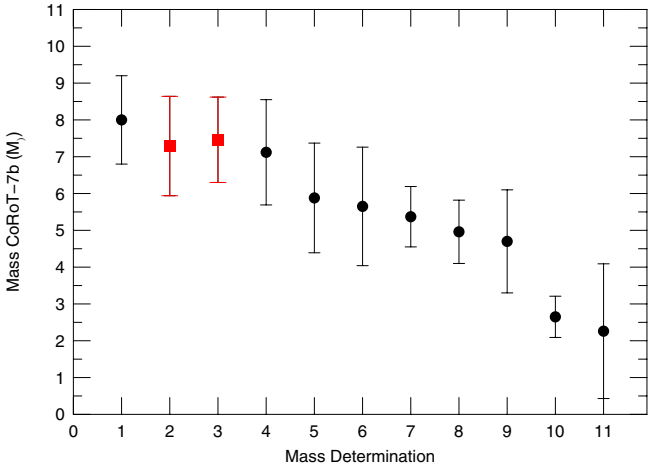

Figure 10. Comparison of the masses for CoRoT-7b that have been reported in the literature. The values on the abscissa correspond to numbers in Table 3. The squares mark the determinations in this work.

(A color version of this figure is available in the online journal.)

was also included. The evolution was characterized via a Gaussian with parameters of peak intensity, epoch, and lifetime. Although this model may be a description of activity of a solar-like star in general it is unclear whether this is a realistic model for this star in particular. A large number of free parameters and assumptions are used to fit integrated quantities. One could imagine that with such a complicated model one can use activity alone to fit the RV variations, including those contributed by the reflex motion due to CoRoT-7b. Furthermore, the Pont et al. result represented an average over all possible spot models considered, but we are concerned with the *K*-amplitude in the presence of the *actual* spot distribution on CoRoT-7. Our approach, on the other hand, has far fewer assumptions and is largely independent of the exact details of the spot distribution and evolution on the star. We consider that our *K*-amplitude determination results in more realistic mass for CoRoT-7b.

4.2. The Mean Density of CoRoT-7b

Given our derived planet mass, we can now estimate the bulk density of the planet. Bruntt et al. (2010) give a planet radius of $1.58 \pm 0.1\, R_\oplus$. This results in a mean planet density of 10.4 ± 1.8 gm cm^{-3}.

The large density of CoRoT-7b has been reinforced by the discovery of a second transiting super-Earth, Kepler-10b (Batalha et al. 2011). Kepler-10b has a slightly smaller mass, $m = 4.56 \pm 1.23\, M_\oplus$ and a smaller radius, $R = 1.416 \pm$

0.0345. (For simplicity, we have taken the mean of the ±error values given in Batalha et al. 2011). However, to within the errors CoRoT-7b and Kepler-10b have identical bulk densities: $\rho_{\rm Kepler-10b} = 8.8 \pm 2.5$ gm cm^{-3} compared to $\rho_{\rm CoRoT-7b} = 10.4 \pm 1.8$ gm cm^{-3}.

What is so striking about these two planets is not only their comparable densities, but that they also orbit very similar host stars (G9V and G4V, respectively) that have a similar radius and mass. The only differences are in the stellar metallicity, Kepler-10 is slightly metal poor with Fe/H] $= -0.15 \pm 0.04$ (Batalha et al. 2011) compared to the CoRoT-7 value of [Fe/H] $= +0.12 \pm 0.06$ (Bruntt et al. 2010), and in the activity level. CoRoT-7 shows relatively high levels of activity, while Kepler-10b is one of the quietest stars in the Kepler sample. This is explained by Kepler-10 also being much older than CoRoT-7, about 8 ± 0.26 Gyr (as derived by asteroseismology). On the other hand, CoRoT-7 has an estimated age of 1.2–2.3 Gyr (Léger et al. 2009). Another similarity between the two systems is that of the very remarkable orbital period of 0.85 day for CoRoT-7b, which was unprecedented for such a low-mass planet, is now mirrored in Kepler-10b with a period of 0.84 day.

Kepler-9d (Holman et al. 2010; Torres et al. 2011) has a similar well-determined radius (≈1.6 $R_\oplus$), a slightly longer period (1.59 days) and an upper mass limit of 7 $M_\oplus$, which, if confirmed, would bring it into the same density regime as CoRoT-7b and Kepler-10b. This is not the case for the small planets recently discovered around the star Kepler-11 (Lissauer et al. 2011), which if their masses are confirmed belong to a type with very much lower densities (≈0.8–2 gm cm^{-3}), so there appears to be a wide range of properties of super-Earth exoplanets. This is also reflected in 55 Cnc-e a recently discovered transiting super-Earth (Winn et al. 2011; Demory et al. 2011). Compared to CoRoT-7b and Kepler-10b, this exoplanet has a larger radius of 2.13 ± 0.14 $R_\oplus$, a comparable mass of 7.98 ± 0.69 $M_\oplus$, but half the density at 4.56 ± 0.99 gm cm^{-3}. This implies the presence of a significant amount of volatiles.

A detailed discussion on the possible internal structure of CoRoT-7b and Kepler-10b is well beyond the scope of this paper. We can, however, compare the density and radius to terrestrial bodies in our own solar system as well as to simple models. The inner terrestrial planets, excluding Mercury, and the Moon show a tight linear correlation between logarithm of the density, ρ, and planet radius, R_P (correlation coefficient, $r = 0.99976$). The terrestrial planets as well as the Moon are shown in Figure 11 along with CoRoT-7b and Kepler-10b. Also shown are three models for a "super-Moon," Earth-like, and a "super-Mercury" (a super-Earth with a structure like Mercury). The Earth-like planet has a silicate mantle that is 67% by mass and an iron core that is 10% by mass. A Moon-like planet has a 100% silicate mantle (MgO and SiO_2) and no core. The Mercury-like planet has an iron core that is 63% of the mass and a silicate mantle that is 37% of the planet mass.

The nominal values of CoRoT-7b and Kepler-10b place these above the Earth-like planets and close to Mercury that is iron enriched. However, within the errors both of these exoplanets have a density and mass consistent with either an Earth-like planet or a super-Mercury. Whether CoRoT-7b and Kepler-10b have an internal structure similar to Mercury or the Earth requires reducing the error on the density. For CoRoT-7b, equal contributions to the error come from the planet mass (19%) and radius (6%, but contributing as R^3 in the density). Kepler-10b benefits from a better measurement of the R_p (due to the asteroseismic determination of the stellar parameters), but the planet mass is known only to within 26%, a bit worse than for CoRoT-7b. A substantial improvement in the mass of Kepler-10b can be realized by a reduction in the K-amplitude error. The RV measurements for Kepler-10b show an rms scatter about the orbit that is a factor of two larger than the internal errors. This is most likely due to the RV jitter of activity (Batalha et al. 2011). This activity jitter is estimated to be about 2 m s^{-1}, or 50% of the planet K-amplitude. So, in order to get a better mass determination for Kepler-10b one would have to correct for the activity signal, even for such a quiet star. Since Kepler-10b has a long rotational period ($P_{\rm rot}$ = 50–100 days), the stellar activity jitter could be reduced by taking several measurements of Kepler-10 throughout the night when the star is well placed in the sky and employing the procedure we used on CoRoT-7b. Unfortunately, the Kepler-10b RV measurements had only two nights where multiple measurements were taken.

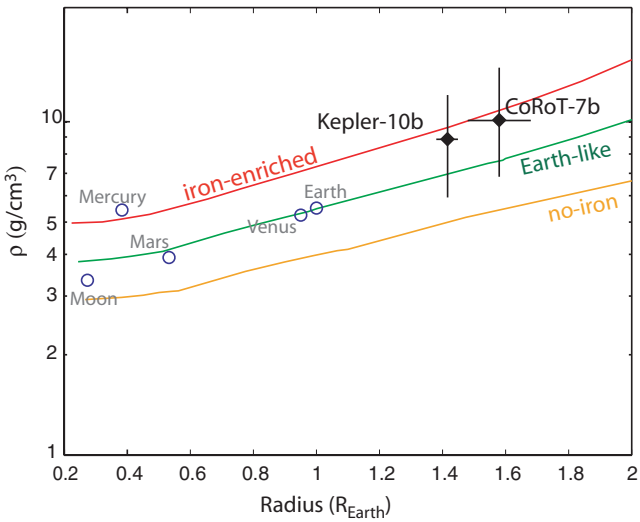

Figure 11. Density–radius relationships for three types of rocky compositions. Earth-like: 67% by mass of silicate mantle with 10% iron by mol [(0.9MgO, 0.1Fe)+SiO_2] + 33% by mass of iron core. No-iron: 100% silicate mantle [MgO + SiO_2 mantle]. Iron enriched: 37% silicate mantle (with 0% of iron by mol) + 63% iron core.

(A color version of this figure is available in the online journal.)

In light of the discovery of Kepler-10b, the properties of CoRoT-7b may not be so extraordinary. It is encouraging that so quickly after the start of the space missions CoRoT and Kepler two transiting rocky planets with comparable (and possibly new) properties have been discovered. This bodes well for the detection of more of such objects.

Figure 11 hints that in terms of structure, CoRoT-7b and Kepler-10b may be more like Mercury than the other terrestrial planets. Clearly, more transiting super-Earths must be found—and with excellent mass and radius determinations—before we know if CoRoT-7b and Kepler-10b just represent a part of the "continuum" of low-mass planets, or whether they are special even among short-period super-Earths.

Not surprisingly, the first confirmed super-Earths found by both CoRoT and Kepler are among the brightest stars in their respective samples. Because they are relatively bright it was possible to get the requisite precise RVs needed to confirm the nature of the transiting object. There are undoubtedly more CoRoT-7b-like planets to be found in the CoRoT and Kepler samples. Unfortunately, these are most likely among the fainter stars of the sample for which the RV determination of the mass is challenging. Clearly, to make significant progress in

the understanding of the CoRoT-7b-type planets it is essential to find such objects around relatively bright stars for which characterization studies are easier. Unfortunately, the requisite precise photometry can only be conducted from space. This only emphasizes the need for such proposed space missions as *PLAnetary Transits and Oscillations* (*PLATO*; see Catala 2009) and the *Transiting Exoplanet Survey Satellite* (*TESS*; see Ricker et al. 2009) whose goals are to find transiting terrestrial planets among the brightest stars. In the case of *PLATO*, stellar parameters will be determined precisely using asteroseismology which translates into more accurate planetary parameters. We will thus be able to determine if the "CoRoT-7b-like" planets are indeed more like Mercury than the Earth in terms of their internal structure.

The German CoRoT Team (Thüringer Landessternwarte and University of Cologne) acknowledges the support of grants 50OW0204, 50OW603, and 50QM1004 from the Deutsches Zentrum für Luft- und Raumfahrt e.V. (DLR). T.M. and G.N. acknowledge the support of the Israel Science Foundation (grant No. 655/07). H.D. and B.T. acknowledge support by grants ESP2007-65480-C02-02 and AYA2010-20982-C02-02 of the Spanish Ministry of Science and Innovation (MICINN). We thank Barbara McArthur for useful discussions regarding *Gaussfit*. Finally, we thank the anonymous referee for critical comments that greatly improved the final manuscript.

REFERENCES

Baglin, A., Auvergne, M., Bosnard, L., et al. 2006, in 36th COSPAR Scientific Assembly, July 16–23, Beijing, China, Meeting abstract from the CDROM 3749
Batalha, N. M., Borucki, W. J., Bryson, S. T., et al. 2011, ApJ, 729, 27
Boisse, I., Bouchy, F., Hébrard, G., et al. 2011, A&A, 528, A4
Bruntt, H., Deleuil, M., Fridlund, M., et al. 2010, A&A, 519, 51
Catala, C. 2009, in Proc. 38th Liege International Astrophysical Colloquium: Evolution and Pulsation of Massive Stars on the Main Sequence and Close to it, Communications in Asteroseismology, Vol.158, ed. A. Noels, C. Aerts, J. Montalban, A. Miglio, & M. Briquet (Vienna: Austrian Academy of Sciences), 330
Demory, B.-O., Gillon, M., Deming, D., et al. 2011, A&A, 533, 114
Ferraz-Mello, S., Tadeu dos Santos, M., Beauge, C., Mitchchenko, T. A., & Rodrigiguez, A. 2011, A&A, 531, 161
Foukal, P. 1987, J. Geophys. Res., 92, 801
Hatzes, A. P. 2002, Astron. Nachr., 323, 392
Hatzes, A. P., Cochran, W. P., Endl, M., et al. 2003, ApJ, 599, 1383
Hatzes, A. P., Dvorak, R., Wucther, G., et al. 2010, A&A, 520, 93
Holman, M. J., Fabrycky, D. C., Ragozzine, D., et al. 2010, Science, 330, 51
Jefferys, W., Fitzpatrick, J., & McArthur, B. 1988, Celest. Mech., 41, 39
Lanza, A. F., Bonomo, A. S., Moutou, C., et al. 2010, A&A, 520, 53
Léger, A., Rouan, D., Schneider, J., et al. 2009, A&A, 506, 287
Lissauer, J. J., Fabrycky, D. C., Ford, E. B., et al. 2011, Nature, 470, 53
Lo Curto, G., Mayor, M., Benz, W., et al. 2010, A&A, 512A, 48L
Mayor, M., Pepe, F., Queloz, D., et al. 2003, Messenger, 114, 20
Moutou, C., Mayor, M., Lo Curto, G., et al. 2011, A&A, 527, 63
Naef, D., Mayor, M., Lo Curto, G., et al. 2010, A&A, 523, 15
Pont, F., Aigrain, S., & Zucker, S. 2011, MNRAS, 411, 1953
Poppenhaeger, K., Lenz, L. F., Reiners, A., Schmitt, J. H. M. M., & Shkolnik, E. 2011, A&A, 528, 58
Poppenhaeger, K., Robrade, J., & Schmitt, J. H. M. M. 2010, A&A, 515, 98
Queloz, D., Bouchy, F., Moutou, C., et al. 2009, A&A, 506, 303
Ricker, G., Latham, D. W., Vanderspek, R. K., et al. 2009, BAAS, 41, 193
Saar, S. H., & Donahue, R. A. 1997, ApJ, 485, 319
Santos, N., Mayor, M., Naef, D., et al. 2002, A&A, 392, 215
Scargle, J. D. 1982, ApJ, 263, 835
Scharf, C. A. 2010, ApJ, 722, 1547
Shkolnik, E., Bohlender, D. A., Walker, G. A. H., & Collier Cameron, A. 2008, ApJ, 676, 628
Shkolnik, E., Walker, G. A. H., Bohlender, D. A., Gu, P.-G., & Kürster, M. 2005, ApJ, 622, 1075
Torres, G., Fressin, F., Batalha, N. M., et al. 2011, ApJ, 727, 24
Valencia, D. 2011, in Detection and Dynamics of Transiting Exoplanets, EPJ Web of Conferences, Vol. 11, ed. F. Bouchy, R. Díaz, & C. Moutou (Les Ulis: EDP Sciences), id.03001
Winn, J. N., Matthews, J. M., Dawson, R. I., et al. 2011, ApJ, 737, L18